etc.

Electrochemistry and Photoelectron Spectra. The apparatus for the electrochemical measurements were described previously.[12] The photoelectron spectra were taken from ref 14 and 15.

Acknowledgment. We wish to thank Dr. M. A. Weiner for some of the photoelectron spectra of metal hydrides and the National Science Foundation for financial support.

Registry No. Me_3SnH, 1631-73-8; n-Bu_3SnH, 688-73-3; n-Bu_3SnD, 6180-99-0; Ph_3SnH, 892-20-6; Et_3GeH, 1188-14-3; n-Bu_3GeH, 998-39-0; Et_3SnH, 997-50-2; Et_3SiH, 617-86-7; i-Pr_3SiH, 6485-79-6; Et_3SiD, 1631-33-0; $Fe(phen)_3(ClO_4)_3$, 14634-90-3; $Fe(5\text{-}Cl\text{-}phen)_3(ClO_4)_3$, 71870-11-6; $Fe(bpy)_3(ClO_4)_3$, 15388-50-8; $Fe(5\text{-}NO_2\text{-}phen)_3(ClO_4)_3$, 53261-42-0; $Fe(4,7\text{-}Ph_2\text{-}phen)_3(ClO_4)_3$, 53204-06-1.

Contribution from the Department of Chemistry,
Stanford University, Stanford, California 94305

Structural Characterization of the Iron-Bridged "Double-Cubane" Cluster Complexes $[Mo_2Fe_7S_8(SC_2H_5)_{12}]^{3-}$ and $[M_2Fe_7S_8(SCH_2C_6H_5)_{12}]^{4-}$ (M = Mo, W) Containing MFe_3S_4 Cores

THOMAS E. WOLFF, JEREMY M. BERG, PHILIP P. POWER, KEITH O. HODGSON, and R. H. HOLM*

Received September 6, 1979

The reaction system $(R'_4N)_2MS_4$ (M = Mo, W)/$FeCl_3$/RSH/NaOMe in methanol or ethanol at ambient temperature has afforded four principal products, $[M_2Fe_6S_9(SR)_8]^{3-}$ (**1**), $[M_2Fe_6S_8(SR)_9]^{3-}$ (**2**), $[M_2Fe_7S_8(SR)_{12}]^{3-}$ (**3**), and $M_2Fe_7S_8(SR)_{12}]^{4-}$ (**4**), which have been isolated as crystalline R'_4N^+ salts. The structures of **1** and **2** (M = Mo; R = Et) have been previously reported and consist of two $MoFe_3S_4(SR)_3$ cubane-type clusters linked through the Mo atoms by (μ-S)(μ-SEt)$_2$ and (μ-SEt)$_3$ bridges, respectively. The structures of **3** (M = Mo, R = Et) and **4** (M = Mo, W; R = CH_2Ph) have been determined by single-crystal X-ray diffraction. $(Me_3NCH_2Ph)_3[Mo_2Fe_7S_8(SEt)_{12}]$ crystallizes in the orthorhombic space group *Pbcn* with a = 32.868 (6) Å, b = 12.922 (2) Å, c = 19.844 (5) Å, and Z = 4. $(n\text{-}Bu_4N)_4[M_2Fe_7S_8(SCH_2Ph)_{12}]$ crystallizes in the monoclinic space group $P2_1/c$ with Z = 2 and a = 15.883 (4) Å, b = 35.035 (7) Å, c = 15.836 (4) Å, and β = 109.20 (2)° (M = Mo) and a = 15.871 (10) Å, b = 34.991 (14) Å, c = 15.814 (8) Å, and β = 109.88 (4)° (M = W). The three anions have an imposed center of symmetry and are of the "double-cubane" type. Each anion contains two $MFe_3S_4(SR)_3$ clusters with trigonally distorted MFe_3S_4 cores which are connected through their M atoms by $M(SR)_3Fe(SR)_3M$ bridging units. The dimensions of the cores do not exhibit any chemically significant differences; those of the Mo and W complexes **4** are essentially indistinguishable and provide a further example of isometric replacement of the two atoms in analogous compounds. The primary dimensional differences reside in the $Fe(SR)_6$ bridge subunits which possess distorted trigonal-antiprismatic coordination. These differences are satisfactorily interpreted in terms of Fe(III) (probably low spin) in **3** and high-spin Fe(II) in **4**, thereby showing that in the couples $[M_2Fe_7S_8(SR)_{12}]^{3-,4-}$ the central Fe atom and not a cluster is the redox site. Whereas the triply bridged units $M[X_3]M$ are common in molybdenum and tungsten chemistry, the "extended" triple bridges in **3** and **4** are the first of this kind to be structurally demonstrated. Other structural features of these anions are also discussed.

Introduction

In the course of our synthetic approach to the molybdenum-containing site in the FeMo proteins of nitrogenase,[1] we are examining reaction system 1 (M = Mo, W) comprised of

$$(R'_4N)_2MS_4 + 3FeCl_3 + 10RSH + 10NaOMe \xrightarrow[\text{EtOH}]{\sim 25\ °C,\ \text{MeOH}} (R'_4N)_3[M_2Fe_6S_9(SR)_8]\ (\mathbf{1}) + (R'_4N)_3[M_2Fe_6S_8(SR)_9]\ (\mathbf{2}) + (R'_4N)_3[M_2Fe_7S_8(SR)_{12}]\ (\mathbf{3}) + (R'_4N)_4[M_2Fe_7S_8(SR)_{12}]\ (\mathbf{4}) \quad (1)$$

elementary reagents. The first products isolated were salts of anions **1**[2,3] and **2**[3] (M = Mo; R = Et). Crystallographic studies have established the indicated "double-cubane" structures in which two clusters containing $MoFe_3S_4$ cores are linked via (μ-S)(μ-SEt)$_2$ (**1**) or (μ-SEt)$_3$ (**2**) bridges between the two Mo atoms. Christou et al.[4,5] have independently prepared other examples of **2** (M = Mo; R = Ph, CH_2CH_2OH), whose structures are essentially isodimensional with that of $[Mo_2Fe_6S_8(SEt)_9]^{3-}$.[3] Structures **1** and **2** are of relevance to the problem of modeling the Mo site in nitrogenase. The extended X-ray absorption fine structure (EXAFS) of the Mo spectra of several FeMo proteins[6] and of the FeMo

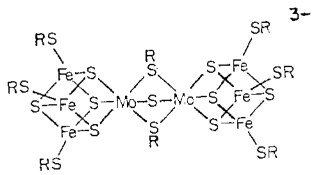

1

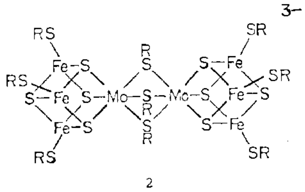

2

---

(1) R. R. Eady and B. E. Smith in "A Treatise on Dinitrogen Fixation", Sections I and II, R. W. F. Hardy, F. Bottomley, and R. C. Burns, Ed., Wiley-Interscience, New York, 1979, Chapter 3 (Section I).

(2) T. E. Wolff, J. M. Berg, C. Warrick, K. O. Hodgson, R. H. Holm, and R. B. Frankel, *J. Am. Chem. Soc.*, **100**, 4630 (1978).

(3) T. E. Wolff, J. M. Berg, K. O. Hodgson, R. B. Frankel, and R. H. Holm, *J. Am. Chem. Soc.*, **101**, 4140 (1979).

(4) G. Christou, C. D. Garner, F. E. Mabbs, and T. J. King, *J. Chem. Soc., Chem. Commun.*, 740 (1978).

(5) G. Christou, C. D. Garner, F. E. Mabbs, and M. G. B. Drew, *J. Chem. Soc., Chem. Commun.*, 91 (1979).

0020-1669/80/1319-0430$01.00/0

Table I. Summary of Crystal Data, Intensity Collection, and Structure Refinement Parameters

data	$(Me_3NCH_2Ph)_3[Mo_2Fe_7S_8(SEt)_{12}]$	$(n\text{-}Bu_4N)_4[Mo_2Fe_7S_8(SCH_2Ph)_{12}]$	$(n\text{-}Bu_4N)_4[W_2Fe_7S_8(SCH_2Ph)_{12}]$
formula	$C_{54}H_{108}Fe_7Mo_2N_3S_{20}$	$C_{148}H_{228}Fe_7Mo_2N_4S_{20}$	$C_{148}H_{228}Fe_7N_4S_{20}W_2$
a, Å	32.868 (6)	15.883 (4)	15.871 (10)
b, Å	12.922 (2)	35.035 (7)	34.991 (14)
c, Å	19.844 (5)	15.836 (4)	15.814 (8)
β, deg		109.90 (2)	109.88 (4)
cryst system	orthorhombic	monoclinic	monoclinic
V, Å^3	8428 (5)	8256 (7)	8259 (15)
Z	4	2	2
d_{calcd}, g/cm^3	1.59	1.30	1.38
d_{obsd}, g/cm^3	1.58[c]	1.29[d]	1.39[d]
space group	*Pbcn*	$P2_1/c$	$P2_1/c$
cryst dimens,[a] mm	0.56 × 0.18 × 0.14	0.36 × 0.26 × 0.20	0.41 × 0.30 × 0.29
cryst faces	$(\bar{3}00)$, $(\bar{3}\bar{1}0)$, $(1\bar{1}0)$ (300), (230), (001) $(00\bar{1})$	$(0\bar{2}\bar{3})$, $(0\bar{3}\bar{2})$, (031) $(03\bar{1})$, (310), $(\bar{3}10)$	$(0\bar{1}1)$, $(\bar{1}00)$, $(01\bar{1})$ $(32\bar{2})$, $(\bar{1}22)$, $(1\bar{6}\bar{2})$
radiation[b]	Mo $K\bar{\alpha}$ (λ 0.710 69 Å)	Mo $K\bar{\alpha}$ (λ 0.710 69 Å)	Mo $K\bar{\alpha}$ (λ 0.710 69 Å)
abs coeff μ, cm^{-1}	19.8	10.4	23.7
transmission factors, %	67.95 min, 77.56 max, 73.37 av	77.12 min, 84.52 max, 81.53 av	48.44 min, 59.19 max, 54.27 av
decay correctn factors			0.9861 min, 1.3273 max, 1.1495 av
takeoff angle, deg	3.0	3.0	3.0
scan speed, deg/min	1.5–29.3 ($\theta/2\theta$ scan)	1.5–29.3 ($\theta/2\theta$ scan)	1.5–29.3 ($\theta/2\theta$ scan)
scan range, deg	0.7 below $K\alpha_1$ to 0.7 above $K\alpha_2$	0.6 below $K\alpha_1$ to 0.6 above $K\alpha_2$	0.7 below $K\alpha_1$ to 0.7 above $K\alpha_2$
bkgd/scan time ratio	0.25	0.25	0.25
data collected	2θ of 2–45° $+h,+k,+l$	2θ of 3–40° $+h,+k,\pm l$	2θ of 3–40° $+h,+k,\pm l$
unique data ($F_o^2 > 3\sigma(F_o^2)$)	2127	4061	5043
no. of variables	393	658	658
error in observn of unit wt	1.61	1.27	1.38
R, %	6.2	4.9	4.6
R_w, %	7.1	5.4	5.5

[a] Irregularly shaped crystals. [b] Mosaic graphite monochromator. [c] Determined by flotation in cyclohexane and saturated $p\text{-}C_6H_4Br_2$ in C_6H_5Br. [d] Determined by flotation in cyclohexane/carbon tetrachloride.

cofactor[7] obtained therefrom[8] has been interpreted in terms of several possible structures in which Mo is surrounded by Fe and S atoms at distances of <3 Å.[6] The Mo EXAFS of $[Mo_2Fe_6S_8(SEt)_9]^{3-}$ and, to a larger degree, that of $[Mo_2Fe_6S_9(SEt)_8]^{3-}$ resembles the Mo EXAFS of the enzyme, suggesting an extent of similarity between the Mo environments in **1** and **2** and in the enzyme. Owing to intrinsic limitations of the technique, the EXAFS results cannot establish the existence of the complete $MoFe_3S_4$ core unit in the enzyme. Nonetheless, the spectral resemblances among the synthetic species and nitrogenase are sufficient to encourage a further pursuit of synthetic Mo–Fe–S cluster species.

We have recently found that alterations in quaternary cation, thiol, and reaction times of system 1 permit the isolation of two new cluster species, the trianions **3** (M = Mo, W; R = Et) and the tetraanions **4** (M = Mo, W; R = CH_2Ph).[9]

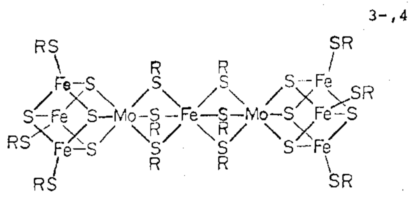

3, 4

These species were found to possess the same overall structure, with two $MFe_3S_4(SR)_6$ clusters bridged by Fe(III) (**3**) or Fe(II) (**4**).[9] Here we report the detailed structures of $(Me_3NCH_2Ph)_3[Mo_2Fe_7S_8(SEt)_{12}]$, $(n\text{-}Bu_4N)_4[Mo_2Fe_7S_8(SCH_2Ph)_{12}]$, and $(n\text{-}Bu_4N)_4[W_2Fe_7S_8(SCH_2Ph)_{12}]$ as a necessary prelude to a future description of their syntheses and physicochemical properties.[10]

Experimental Section

Suitable crystals of $(Me_3NCH_2Ph)_3[Mo_2Fe_7S_8(SEt)_{12}]$ and $(n\text{-}Bu_4N)_4[M_2Fe_7S_8(SCH_2Ph)_{12}]$ (M = Mo, W) were produced by anaerobic recrystallization from acetonitrile solutions. The three compounds were obtained from reaction system 1 as briefly described;[9] full details of synthetic procedures will be reported elsewhere.[10]

Collection and Reduction of X-ray Data. Crystals were mounted in glass capillaries under an argon atmosphere. Diffraction experiments were performed on a Syntex $P2_1$ four-circle diffractometer with a Mo X-ray tube equipped with a graphite monochromator. The machine parameters are summarized in Table I. In each case an orientation matrix was determined and refined by using 15 reflections which had 2θ values between 14 and 20°. Each crystal showed several ω scans with full width at half-height less than 0.25°.

The parameters relevant to X-ray data collections are listed in Table I. Throughout each data collection, three standard reflections were monitored every 60 reflections. For $(Me_3NCH_2Ph)_3[Mo_2Fe_7S_8(SEt)_{12}]$ and $(n\text{-}Bu_4N)_4[Mo_2Fe_7S_8(SCH_2Ph)_{12}]$ no significant variation was observed. However, a steady decrease of ca. 10% in intensity of the standard reflections of $(n\text{-}Bu_4N)_4[W_2Fe_7S_8(SCH_2Ph)_{12}]$ necessitated the application of an anisotropic decay correction based on the standard reflections. The diffraction data were processed as described previously.[11] Analytical absorption corrections were applied to all three data sets. In all cases the systematic absences uniquely determined the space group. $(Me_3NCH_2Ph)_3[Mo_2Fe_7S_8(SEt)_{12}]$ belongs to the orthorhombic crystal system with systematic absences $0kl$ ($k \neq 2n$), $h0l$ ($l \neq 2n$), and $hk0$ ($h + k \neq 2n$), which indicate that the space group is *Pbcn*. The compounds $(n\text{-}Bu_4N)_4[M_2Fe_7S_8(SCH_2Ph)_{12}]$ (M = Mo, W) are isomorphous and belong to the monoclinic crystal system. The systematic absences $0k0$ (k

---

(6) S. P. Cramer, K. O. Hodgson, W. O. Gillum, and L. E. Mortenson, *J. Am. Chem. Soc.*, **100**, 3398 (1978).

(7) S. P. Cramer, W. O. Gillum, K. O. Hodgson, L. E. Mortenson, E. I. Stiefel, J. R. Chisnell, W. J. Brill, and V. K. Shah, *J. Am. Chem. Soc.*, **100**, 3814 (1978).

(8) V. K. Shah and W. J. Brill, *Proc. Natl. Acad. Sci. USA*, **74**, 3249 (1977).

(9) T. E. Wolff, J. M. Berg, P. P. Power, K. O. Hodgson, R. H. Holm, and R. B. Frankel, *J. Am. Chem. Soc.*, **101**, 5454 (1979).

(10) P. P. Power, T. E. Wolff, R. B. Frankel, and R. H. Holm, results to be submitted for publication.

(11) M. A. Bobrik, K. O. Hodgson, and R. H. Holm, *Inorg. Chem.*, **16**, 1851 (1977). This paper contains a listing of the computer programs used in the X-ray diffraction studies reported here.

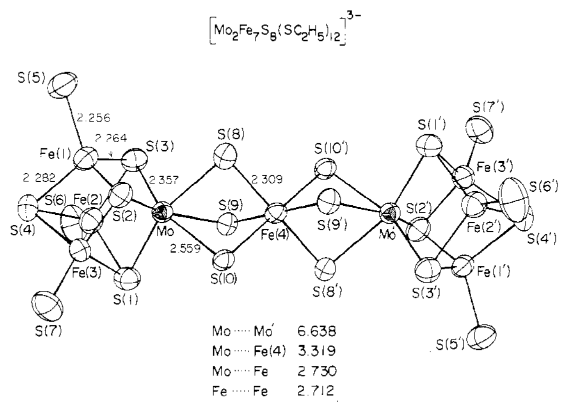

Figure 1. Structure of $[Mo_2Fe_7S_8(SEt)_{12}]^{3-}$, showing 50% probability ellipsoids, the atom labeling scheme, and selected mean interatomic distances; not included are the 12 ethyl groups of the bridging and terminal thiolate ligands.

$\neq 2n$) and $h0l$ ($l \neq 2n$) are consistent only with the space group $P2_1/c$. Subsequent solution and refinement of the structures confirmed these space group assignments.

Solution and Refinement of the Structures. The structures were solved by using the direct methods program MULTAN. In $(Me_3NCH_2Ph)_3[Mo_2Fe_7S_8(SEt)_{12}]$ and $(n\text{-}Bu_4N)_4[Mo_2Fe_7S_8(SCH_2Ph)_{12}]$, trial positions for the Mo, Fe, and S atoms were determined from an E map. The remaining nonhydrogen atoms were located from subsequent difference Fourier maps. Atom coordinates for $(n\text{-}Bu_4N)_4[W_2Fe_7S_8(SCH_2Ph)_{12}]$ were taken directly from the analogous Mo structure and were refined in an identical manner.

In all three structures the asymmetric unit consists of half of the anion and the corresponding number of cations. The anions each have a crystallographically imposed inversion center and were fully refined anisotropically. The cations of $(Me_3NCH_2Ph)_3[Mo_2Fe_7S_8(SEt)_{12}]$ are situated such that the asymmetric unit contains 1.5 cations; one of these lies in a general position and was refined anisotropically, while the second is disordered about a twofold axis passing approximately through the nitrogen atom and the center of the phenyl ring. The second cation was best refined, however, by placing atoms N(2), C(5)N(2), and C(8)N(2) (See Table VII[12]) on the twofold axis and refining the ring carbon atoms anisotropically to account for the artificial placement of these atoms. The asymmetric unit of $(n\text{-}Bu_4N)_4[M_2Fe_7S_8(SCH_2Ph)_{12}]$ contains two independent cations. All atoms are well-ordered except for one methyl carbon. Three positions, labeled C(16)N(1), C(17)N(1), and C(18)N(1) in the tables, were found for this atom and the multiplicities of these atom positons were refined such that the total occupancy was one. For all three structures, hydrogen atoms were calculated only when their positions were well determined by the structure. Standard geometries and C–H bond distances of 0.95 Å were assumed, and temperature factors were set to values comparable to those of the neighboring carbon atoms. The hydrogen atoms were included as fixed contributions in the final refinement cycles. Final difference Fourier maps showed no peaks with height greater than ca. 25% of that of a carbon atom.

The following results are tabulated: positional and thermal parameters for Fe, S, and Mo or W atoms of the anions (Table II); selected interatomic distances and angles in the anions (Table III); best weighted least-squares planes for two anions (Table IV); root-mean-square amplitudes of thermal vibration of the anions (Table V); positional and thermal parameters for thiolate carbon atoms of the anions (Table VI[12]) and for nitrogen and carbon atoms of the cations (Table VII[12]); values of $10|F_o|$ and $10|F_c|$ for each structure (Tables VIII–X[12]). Structures of the anions are presented in Figures 1–3.

Results and Discussion

From Figures 1–3 the structures of $[Mo_2Fe_7S_8(SEt)_{12}]^{3-}$, $[Mo_2Fe_7S_8(SCH_2Ph)_{12}]^{4-}$, and $[W_2Fe_7S_8(SCH_2Ph)_{12}]^{4-}$ are seen to be of the "double-cubane" type **3** and **4**. A stereoview of $[Mo_2Fe_7S_8(SCH_2Ph)_{12}]^{4-}$ is provided in Figure 4. The $MFe_3S_4(SR)_3$ clusters, containing MFe_3S_4 cores, are linked through their M atoms by a $Fe(SR)_6$ bridge subunit. Equivalently, two $MFe_3S_4(SR)_6$ clusters act as tridentate ligands to Fe(III) (**3**) or Fe(II) (**4**), resulting in trigonally distorted octahedral coordination about the central Fe atom. The compounds $(n\text{-}Bu_4N)_4[M_2Fe_7S_8(SCH_2Ph)_{12}]$ (M = Mo, W) both crystallize in the monoclinic space group $P2_1/c$ with isomorphous unit cells. $(Me_3NCH_2Ph)_3[Mo_2Fe_7S_8(SEt)_{12}]$ crystallizes in the orthorhombic space group $Pbcn$. From the crystal data (Table I) the only symmetry imposed on each anion is centrosymmetry. This situation differs from that of the previously studied compounds containing $[Mo_2Fe_6S_9(SEt)_8]^{3-}$ [2,3] (**1**) and $[Mo_2Fe_6S_8(SEt)_9]^{3-}$ [3] (**2**), where actual or apparent trigonal symmetry is crystallographically imposed on the anions. Thus the present set of compounds affords an opportunity to examine any deviations of the anions from trigonal symmetry.[13] The format for description of the three anion structures follows that employed earlier.[3] In describing these structures, clusters and bridging units are examined in turn, with attention directed to the bond distances and angles in Table III and the least-squares planes in Table IV. Each structure consists of discrete anions and cations. Structural features of R substituents and cations are unexceptional and are not described.

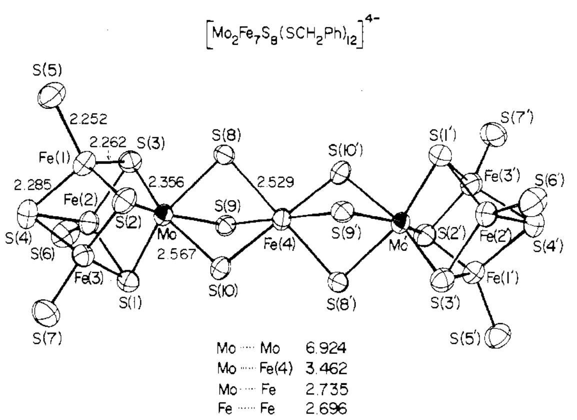

Figure 2. Structure of $[Mo_2Fe_7S_8(SCH_2Ph)_{12}]^{4-}$, showing 50% probability ellipsoids, the atom labeling scheme, and selected mean interatomic distances; not included are the 12 benzyl groups of the bridging and terminal thiolate ligands.

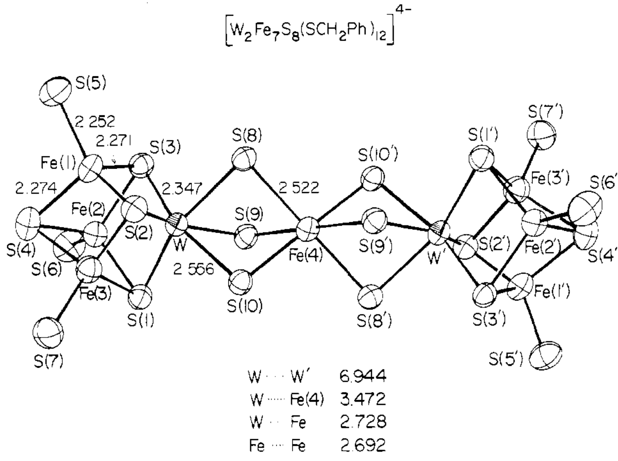

Figure 3. Structure of $[W_2Fe_7S_8(SCH_2Ph)_{12}]^{4-}$, showing 50% probability ellipsoids, the atom labeling scheme, and selected mean interatomic distances; not included are the 12 benzyl groups of the bridging and terminal thiolate ligands.

---

[12] Supplementary material.

[13] The same opportunity is afforded by $(n\text{-}Bu_4N)_3[Mo_2Fe_6S_8(SPh)_9]$ but cannot be pursued at this time owing to the availability of only mean distances in the structure refined to $R = 8.8\%$.[4]

Table II. Positional and Thermal Parameters[a] for $[Mo_2Fe_7S_8(SEt)_{12}]^{3-}$ and $[M_2Fe_7S_8(SCH_2Ph)_{12}]^{4-}$ (M = Mo, W)

atom	x	y	z	B_{11}[b]	B_{22}	B_{33}	B_{12}	B_{13}	B_{23}
$(Me_3NCH_2Ph)_3[Mo_2Fe_7S_8(SEt)_{12}]$									
Mo	0.08155 (5)[c]	−0.1509 (1)	0.00881 (8)	2.98 (7)	3.48 (7)	2.78 (7)	0.15 (8)	0.22 (8)	0.06 (8)
Fe(1)	0.13147 (9)	−0.2633 (2)	0.0919 (2)	3.6 (1)	4.4 (2)	3.8 (1)	0.2 (1)	−0.4 (1)	0.7 (1)
Fe(2)	0.11746 (10)	−0.3288 (3)	−0.0362 (2)	4.6 (2)	4.6 (2)	4.3 (1)	0.6 (2)	0.6 (1)	−0.3 (1)
Fe(3)	0.16283 (8)	−0.1582 (2)	−0.0152 (1)	3.2 (1)	5.2 (2)	4.3 (1)	0.3 (1)	0.7 (1)	0.6 (2)
Fe(4)	0.00000 (0)	0.0000 (0)	0.0000 (0)	2.9 (2)	3.9 (2)	2.2 (2)	−0.1 (2)	0.2 (2)	0.1 (2)
S(1)	0.1142 (2)	−0.1782 (5)	−0.0950 (3)	4.8 (3)	5.1 (3)	3.2 (2)	0.3 (3)	0.7 (2)	−0.3 (3)
S(2)	0.1346 (2)	−0.0897 (4)	0.0788 (3)	3.8 (3)	4.7 (3)	3.8 (3)	0.0 (3)	0.1 (2)	−0.6 (3)
S(3)	0.0718 (2)	−0.3208 (4)	0.0488 (3)	4.3 (3)	4.1 (3)	4.2 (3)	−0.5 (3)	−0.1 (2)	0.3 (2)
S(4)	0.1790 (2)	−0.3220 (5)	0.0186 (3)	3.9 (3)	5.3 (3)	6.0 (3)	1.7 (2)	0.4 (3)	0.9 (3)
S(5)	0.1409 (2)	−0.3049 (5)	0.2015 (3)	6.6 (4)	5.6 (3)	3.9 (3)	0.6 (3)	−0.7 (3)	0.5 (3)
S(6)	0.1139 (2)	−0.4563 (5)	−0.1135 (4)	9.6 (5)	6.2 (4)	7.6 (4)	2.4 (4)	−1.5 (4)	−2.6 (3)
S(7)	0.2134 (2)	−0.0710 (5)	−0.0667 (3)	4.1 (3)	7.3 (4)	5.9 (3)	−1.1 (3)	0.8 (3)	0.5 (3)
S(8)	0.0279 (2)	−0.0843 (4)	0.0922 (2)	3.0 (3)	4.5 (3)	2.6 (2)	0.3 (2)	0.4 (2)	0.3 (2)
S(9)	0.0138 (2)	−0.1546 (4)	−0.0539 (2)	3.5 (2)	3.9 (3)	3.2 (2)	0.2 (2)	0.0 (2)	−0.6 (2)
S(10)	0.0670 (2)	0.0374 (4)	−0.0229 (2)	3.3 (2)	4.4 (3)	2.7 (2)	0.3 (2)	−0.4 (2)	−0.3 (2)
$(n\text{-}Bu_4N)_4[Mo_2Fe_7S_8(SCH_2Ph)_{12}]$									
Mo	0.61223 (7)	0.08572 (3)	0.51348 (6)	3.01 (4)	2.19 (4)	2.87 (4)	−0.07 (4)	0.99 (3)	−0.07 (4)
Fe(1)	0.5955 (1)	0.16365 (5)	0.4993 (1)	4.29 (8)	2.65 (8)	3.78 (8)	0.26 (7)	1.52 (6)	0.21 (7)
Fe(2)	0.7298 (1)	0.12889 (5)	0.4611 (1)	3.82 (7)	3.28 (8)	3.60 (7)	−0.31 (8)	1.64 (6)	−0.04 (7)
Fe(3)	0.7329 (1)	0.13202 (5)	0.6321 (1)	3.72 (8)	3.21 (8)	3.35 (7)	−0.11 (7)	0.92 (6)	−0.20 (7)
Fe(4)	0.5000 (0)	0.00000 (0)	0.5000 (0)	3.6 (1)	2.5 (1)	3.6 (1)	−0.5 (1)	1.18 (9)	−0.1 (1)
S(1)	0.7691 (2)	0.08126 (9)	0.5634 (2)	3.1 (1)	3.5 (2)	3.9 (1)	0.1 (1)	1.1 (1)	0.2 (1)
S(2)	0.5853 (2)	0.12870 (9)	0.6156 (2)	4.3 (1)	3.1 (1)	3.7 (1)	0.2 (1)	1.9 (1)	0.0 (1)
S(3)	0.5827 (2)	0.12367 (9)	0.3830 (2)	4.0 (1)	3.7 (2)	3.0 (1)	0.0 (1)	1.1 (1)	0.5 (1)
S(4)	0.7412 (2)	0.18304 (9)	0.5445 (2)	5.2 (2)	3.0 (1)	4.4 (1)	−0.9 (1)	1.9 (1)	−0.5 (1)
S(5)	0.5024 (2)	0.21415 (10)	0.4662 (2)	5.8 (2)	3.6 (2)	6.0 (2)	1.0 (2)	1.7 (1)	0.3 (2)
S(6)	0.8162 (2)	0.13397 (10)	0.3747 (2)	6.2 (2)	5.3 (2)	6.2 (2)	1.0 (2)	3.9 (1)	1.2 (2)
S(7)	0.8255 (2)	0.14255 (10)	0.7738 (2)	4.7 (2)	4.8 (2)	4.2 (2)	−0.1 (2)	0.2 (1)	−0.9 (1)
S(8)	0.4446 (2)	0.06875 (9)	0.4599 (2)	2.9 (1)	3.5 (2)	3.2 (1)	−0.1 (1)	0.8 (1)	0.2 (1)
S(9)	0.6009 (2)	0.02523 (8)	0.4192 (2)	2.9 (1)	3.0 (1)	3.4 (1)	0.3 (1)	1.1 (1)	−0.4 (1)
S(10)	0.6176 (2)	0.03228 (8)	0.6260 (2)	4.0 (1)	2.8 (1)	2.9 (1)	0.0 (1)	1.3 (1)	0.1 (1)
$(n\text{-}Bu_4N)_4[W_2Fe_7S_8(SCH_2Ph)_{12}]$									
W	0.61296 (3)	0.08601 (1)	0.51344 (3)	3.46 (2)	2.48 (2)	3.01 (2)	−0.02 (3)	1.20 (1)	0.02 (3)
Fe(1)	0.5965 (1)	0.16380 (5)	0.4993 (1)	4.82 (9)	2.85 (8)	4.17 (8)	0.15 (8)	1.78 (6)	0.21 (8)
Fe(2)	0.7310 (1)	0.12899 (5)	0.4615 (1)	4.46 (8)	3.42 (9)	3.88 (8)	−0.33 (8)	1.75 (6)	−0.20 (8)
Fe(3)	0.7332 (1)	0.13210 (5)	0.6323 (1)	4.38 (8)	3.41 (9)	3.79 (8)	−0.23 (8)	1.37 (7)	−0.25 (8)
Fe(4)	0.5000 (0)	0.00000 (0)	0.5000 (0)	4.1 (1)	3.1 (1)	3.6 (1)	−0.2 (1)	1.40 (9)	−0.1 (1)
S(1)	0.7690 (2)	0.08058 (9)	0.5632 (2)	4.0 (1)	3.3 (2)	4.1 (1)	0.0 (1)	1.4 (1)	0.0 (1)
S(2)	0.5854 (2)	0.12863 (10)	0.6155 (2)	4.3 (1)	3.6 (2)	4.0 (1)	0.2 (1)	1.9 (1)	0.0 (1)
S(3)	0.5831 (2)	0.12349 (10)	0.3827 (2)	4.3 (1)	3.5 (2)	3.5 (1)	−0.1 (1)	1.4 (1)	0.7 (1)
S(4)	0.7417 (2)	0.18281 (10)	0.5445 (2)	5.9 (2)	3.1 (2)	4.9 (2)	−0.9 (1)	2.2 (1)	−0.5 (1)
S(5)	0.5027 (3)	0.21421 (11)	0.4659 (3)	6.6 (2)	4.1 (2)	6.0 (2)	1.4 (2)	2.0 (2)	0.4 (2)
S(6)	0.8177 (3)	0.13377 (12)	0.3751 (2)	7.1 (2)	5.9 (2)	6.1 (2)	0.9 (2)	4.2 (1)	1.0 (2)
S(7)	0.8256 (3)	0.14231 (11)	0.7743 (2)	5.3 (2)	4.9 (2)	4.3 (2)	−0.2 (2)	0.9 (1)	−1.1 (2)
S(8)	0.4465 (2)	0.06876 (9)	0.4606 (2)	3.9 (2)	3.5 (2)	3.4 (1)	0.1 (1)	1.1 (1)	0.5 (1)
S(9)	0.6011 (2)	0.02545 (9)	0.4197 (2)	4.1 (1)	2.8 (2)	3.6 (1)	0.1 (1)	1.3 (1)	−0.4 (1)
S(10)	0.6174 (2)	0.03263 (10)	0.6251 (2)	4.2 (2)	3.3 (2)	3.2 (1)	0.0 (1)	1.3 (1)	0.3 (1)

[a] Data for Mo, W, Fe, and S atoms only. [b] The form of the anisotropic thermal parameter is $\exp[-{}^1/_4(B_{11}h^2a^{*2} + B_{22}k^2b^{*2} + B_{33}l^2c^{*2} + 2B_{12}hka^*b^* + 2B_{13}hla^*c^* + 2B_{23}klb^*c^*)]$. [c] Estimated standard deviations in parentheses in this and succeeding tables.

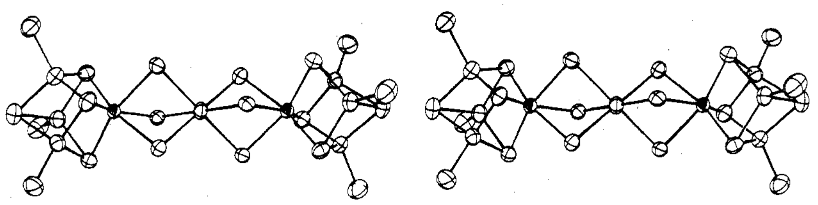

Figure 4. Stereoview of $[Mo_2Fe_7S_8(SCH_2Ph)_{12}]^{4-}$, showing 50% probability ellipsoids. Benzyl groups are omitted for clarity.

A. $MFe_3S_4(SR)_3$ Clusters. The following are the principal structural features of these clusters. (1) The MFe_3S_4 cores are composed of two interlocking imperfect tetrahedra (MFe_3, S_4), of which the S_4 tetrahedron has the larger volume. (2) The $MoFeS_2$ and Fe_2S_2 core faces (planes 1–6) are distinctly nonplanar rhombs. (3) Core diagonal planes 7–12 are nearly perfect.[14] (4) The cores exhibit a dominant trigonal distortion from cubic symmetry, as expected from the presence of MFe_3 subunits. This distortion is most strongly reflected by a compression of S_4 tetrahedra along the idealized threefold axis, which passes through M and S(4). In $[Mo_2Fe_7S_8(SEt)_{12}]^{3-}$, for example, the three S···S distances perpendicular to this axis average to 3.682 (11) Å whereas the mean value of the three remaining S···S distances is 3.578 (35) Å. Similar differences are found in $[M_2Fe_7S_8(SCH_2Ph)_{12}]^{4-}$, where within 3$\sigma$ uncertainty S···S distances divide into sets of three long and three short. (5) A small rhombic distortion is present in

---

(14) Planes of $[W_2Fe_7S_8(SCH_2Ph)_{12}]^{4-}$ are omitted from Table IV because they are virtually identical with those of its Mo analogue.

Table III. Selected Interatomic Distances (Å) and Angles (Deg) in $[Mo_2Fe_7S_8(SEt)_{12}]^{3-}$ and $[M_2Fe_7S_8(SCH_2Ph)_{12}]^{4-}$ (M = Mo, W)

	$[Mo_2Fe_7S_8(SEt)_{12}]^{3-}$	$[Mo_2Fe_7S_8(SCH_2Ph)_{12}]^{4-}$	$[W_2Fe_7S_8(SCH_2Ph)_{12}]^{4-}$
Bridge Units			
M· · ·M′[b]	6.638 (2)	6.924 (1)	6.944 (2)
M· · ·Fe(4)	3.319 (1)	3.462 (1)	3.472 (2)
M–S(8)	2.567 (4)	2.574 (3)	2.557 (12)
M–S(9)	2.551 (4)	2.563 (3)	2.556 (11)
M–S(10)	2.558 (5)	2.565 (3)	2.555 (11)
mean	2.559 (8)[a]	2.567 (6)	2.556 (1)
Fe(4)–S(8)	2.317 (4)	2.569 (3)	2.557 (11)
Fe(4)–S(9)	2.310 (4)	2.526 (3)	2.522 (11)
Fe(4)–S(10)	2.300 (5)	2.492 (3)	2.486 (11)
mean	2.309 (9)	2.529 (39)	2.522 (36)
S(8)–M–S(9)	73.8 (1)	75.94 (9)	75.5 (4)
S(8)–M–S(10)	73.2 (2)	81.18 (9)	80.5 (4)
S(9)–M–S(10)	74.6 (2)	77.30 (9)	76.9 (4)
mean	73.9	78.1	77.6
M–S(8)–Fe(4)	85.5 (1)	84.62 (9)	85.5 (4)
M–S(9)–Fe(4)	86.0 (1)	85.72 (9)	86.3 (4)
M–S(10)–Fe(4)	86.0 (2)	86.37 (9)	87.1 (4)
mean	85.8	85.6	86.3
S(8)–Fe(4)–S(9)	83.2 (2)	76.68 (9)	76.1 (4)
S(8)–Fe(4)–S(10)	82.9 (2)	82.69 (9)	81.9 (4)
S(9)–Fe(4)–S(10)	84.4 (2)	79.32 (9)	78.8 (4)
mean	83.5	79.6	78.9
S(8)–Fe(4)–S(9′)	96.8 (2)	103.32 (9)	103.9 (4)
S(8)–Fe(4)–S(10′)	97.1 (2)	97.31 (9)	98.1 (4)
S(9)–Fe(4)–S(10′)	95.6 (2)	100.68 (9)	101.2 (4)
mean	96.5	100.4	101.0
S(8)· · ·S(9)	3.072 (6)	3.161 (4)	3.132 (16)
S(8)· · ·S(10)	3.056 (6)	3.344 (4)	3.305 (15)
S(9)· · ·S(10)	3.096 (6)	3.203 (4)	3.179 (15)
mean	3.075 (20)	3.236 (96)	3.205 (89)
S(8)· · ·S(9′)	3.461 (6)	3.996 (4)	3.999 (16)
S(8)· · ·S(10′)	3.461 (6)	3.800 (4)	3.810 (16)
S(9)· · ·S(10′)	3.415 (6)	3.863 (4)	3.870 (16)
mean	3.446 (27)	3.886 (10)	3.893 (97)
Clusters			
M–S(1)	2.350 (5)	2.349 (3)	2.337 (11)
M–S(2)	2.364 (5)	2.353 (3)	2.346 (11)
M–S(3)	2.356 (5)	2.366 (3)	2.357 (11)
mean	2.357 (7)	2.356 (9)	2.347 (10)
M· · ·S(4)	3.896 (5)	3.921 (3)	3.900 (12)
S(1)–M–S(9)	88.2 (2)	89.8 (1)	89.4 (4)
S(1)–M–S(10)	90.7 (2)	86.4 (1)	86.0 (4)
S(2)–M–S(8)	90.9 (2)	88.0 (1)	87.8 (4)
S(2)–M–S(10)	87.9 (2)	87.8 (1)	87.5 (4)
S(3)–M–S(8)	90.1 (2)	88.1 (1)	88.2 (4)
S(3)–M–S(9)	91.6 (2)	90.1 (1)	90.0 (4)
mean	89.9	88.4	88.2
S(1)–M–S(2)	103.2 (2)	103.4 (1)	104.1 (4)
S(1)–M–S(3)	102.6 (2)	101.7 (1)	102.4 (4)
S(2)–M–S(3)	102.4 (2)	102.3 (1)	102.8 (4)
mean	102.7	102.5	103.1
M· · ·Fe(1)	2.742 (3)	2.745 (2)	2.736 (6)
M· · ·Fe(2)	2.733 (3)	2.742 (2)	2.738 (6)
M· · ·Fe(3)	2.715 (3)	2.717 (2)	2.709 (6)
mean	2.730 (14)	2.735 (15)	2.728 (16)
Fe(1)· · ·Fe(2)	2.718 (4)	2.697 (2)	2.697 (9)
Fe(1)· · ·Fe(3)	2.725 (4)	2.699 (2)	2.694 (9)
Fe(2)· · ·Fe(3)	2.693 (4)	2.693 (2)	2.693 (9)
mean	2.712 (17)	2.696 (3)	2.695 (2)
Fe(1)–M–Fe(2)	59.53 (8)	58.89 (5)	59.0 (2)
Fe(1)–M–Fe(3)	59.91 (8)	59.23 (5)	59.3 (2)
Fe(2)–M–Fe(3)	59.25 (9)	59.13 (5)	59.3 (2)
mean	59.56	59.1	59.2
Clusters (*continued*)			
M–Fe(1)–Fe(2)	60.07 (9)	60.50 (5)	60.5 (2)
M–Fe(1)–Fe(3)	59.56 (8)	59.87 (5)	59.8 (2)
M–Fe(2)–Fe(1)	60.40 (8)	60.61 (5)	60.5 (2)
M–Fe(2)–Fe(3)	60.05 (8)	59.97 (5)	59.8 (2)
M–Fe(3)–Fe(1)	60.53 (8)	60.90 (5)	60.9 (2)
M–Fe(3)–Fe(2)	60.70 (9)	60.90 (5)	60.9 (2)
mean	60.22	60.46	60.4
Fe(2)–Fe(1)–Fe(3)	59.31 (10)	59.88 (6)	59.9 (2)
Fe(1)–Fe(2)–Fe(3)	60.48 (9)	60.09 (6)	60.0 (2)
Fe(1)–Fe(3)–Fe(2)	60.21 (10)	60.02 (6)	60.1 (2)
mean	60.00	60.00	60.0
Fe(1)–S(2)	2.260 (5)	2.263 (3)	2.267 (13)
Fe(1)–S(3)	2.266 (5)	2.268 (3)	2.274 (13)
Fe(2)–S(1)	2.272 (6)	2.260 (3)	2.272 (13)
Fe(2)–S(3)	2.261 (5)	2.249 (3)	2.261 (13)
Fe(3)–S(1)	2.264 (5)	2.259 (3)	2.278 (13)
Fe(3)–S(2)	2.264 (5)	2.272 (3)	2.272 (13)
mean	2.264 (4)	2.262 (8)	2.271 (6)
Fe(1)–S(4)	2.265 (6)	2.280 (4)	2.269 (14)
Fe(2)–S(4)	2.297 (6)	2.283 (3)	2.269 (13)
Fe(3)–S(4)	2.283 (6)	2.293 (3)	2.285 (13)
mean	2.282 (16)	2.285 (7)	2.274 (9)
mean of 9	2.270 (12)	2.270 (14)	2.272 (7)
M–S(1)–Fe(2)	72.5 (2)	72.96 (10)	72.9 (4)
M–S(1)–Fe(3)	72.1 (2)	72.21 (10)	71.9 (4)
M–S(2)–Fe(1)	72.7 (2)	72.95 (9)	72.7 (4)
M–S(2)–Fe(3)	71.8 (2)	71.93 (9)	71.8 (4)
M–S(3)–Fe(1)	72.8 (2)	72.61 (9)	72.4 (4)
M–S(3)–Fe(2)	72.6 (2)	72.85 (10)	72.7 (4)
mean	72.4	72.6	72.4
S(2)–Fe(1)–S(3)	108.7 (2)	108.4 (1)	108.0 (5)
S(1)–Fe(2)–S(3)	108.3 (2)	108.4 (1)	107.6 (5)
S(1)–Fe(3)–S(2)	109.3 (2)	109.1 (1)	108.5 (5)
mean	108.9	108.6	108.0
S(2)–Fe(1)–S(4)	103.2 (2)	104.6 (1)	104.7 (5)
S(3)–Fe(1)–S(4)	104.2 (2)	103.9 (1)	104.0 (5)
S(1)–Fe(2)–S(4)	104.6 (2)	104.5 (1)	105.0 (5)
S(3)–Fe(2)–S(4)	103.3 (2)	104.4 (1)	104.4 (5)
S(1)–Fe(3)–S(4)	105.3 (2)	104.2 (1)	104.3 (5)
S(2)–Fe(3)–S(4)	102.4 (2)	103.9 (1)	104.0 (5)
mean	103.8	104.3	104.4
mean of 9	105.5	105.7	105.7
Fe(1)–S(5)	2.261 (6)	2.251 (4)	2.252 (14)
Fe(2)–S(6)	2.254 (6)	2.250 (3)	2.249 (14)
Fe(3)–S(7)	2.253 (6)	2.256 (3)	2.254 (13)
mean	2.256 (4)	2.252 (3)	2.252 (3)
S(2)–Fe(1)–S(5)	109.9 (2)	113.0 (1)	112.9 (5)
S(3)–Fe(1)–S(5)	113.8 (2)	115.2 (1)	115.1 (5)
S(1)–Fe(2)–S(6)	105.9 (2)	114.7 (1)	114.5 (5)
S(3)–Fe(2)–S(6)	120.5 (3)	114.0 (1)	114.0 (5)
S(1)–Fe(3)–S(7)	105.1 (2)	114.9 (1)	114.8 (5)
S(2)–Fe(3)–S(7)	118.8 (2)	114.9 (1)	114.9 (5)
mean	112.3	114.5	114.4
S(4)–Fe(1)–S(5)	116.4 (2)	110.8 (1)	111.4 (5)
S(4)–Fe(2)–S(6)	113.3 (3)	110.0 (1)	110.4 (6)
S(4)–Fe(3)–S(7)	115.2 (2)	108.8 (1)	109.2 (5)
mean	114.9	109.9	110.3
mean of 9	113.2	113.0	113.0
Fe(1)· · ·S(1)	3.910 (5)	3.881 (3)	3.888 (13)
Fe(2)· · ·S(2)	3.880 (5)	3.883 (3)	3.887 (13)
Fe(3)· · ·S(3)	3.871 (5)	3.864 (3)	3.867 (12)
mean	3.887 (20)	3.876 (10)	3.881 (12)

Table III (*Continued*)

S(1)· · ·S(2)	3.694 (6)	3.690 (4)	3.693 (16)
S(1)· · ·S(3)	3.673 (6)	3.658 (4)	3.658 (16)
S(2)· · ·S(3)	3.678 (6)	3.674 (4)	3.675 (16)
mean	3.682 (11)	3.674 (16)	3.675 (18)
S(1)· · ·S(4)	3.615 (7)	3.593 (4)	3.603 (16)
S(2)· · ·S(4)	3.545 (7)	3.594 (4)	3.592 (17)
S(3)· · ·S(4)	3.574 (7)	3.581 (4)	3.580 (16)
mean	3.578 (35)	3.589 (7)	3.592 (12)
mean of 6	3.630 (61)	3.632 (48)	3.634 (48)
Fe(2)–S(1)–Fe(3)	72.8 (2)	73.2 (1)	72.6 (4)
Fe(1)–S(2)–Fe(3)	74.1 (2)	73.1 (1)	72.8 (4)
Fe(1)–S(3)–Fe(2)	73.8 (2)	73.3 (1)	73.0 (4)
mean	73.6	73.2	72.8
Fe(1)–S(4)–Fe(2)	73.1 (2)	72.5 (1)	72.9 (4)
Fe(1)–S(4)–Fe(3)	73.6 (2)	72.4 (1)	72.5 (4)
Fe(2)–S(4)–Fe(3)	72.0 (2)	72.1 (1)	72.5 (4)
mean	72.9	72.3	72.6
mean of 6	73.2	72.8	72.7

[a] The standard deviation of the mean was estimated from $\sigma \approx s = [(\Sigma x_i^2 - n\bar{x}^2)/(n-1)]^{1/2}$; no value is given for any angular quantity, as the variations exceed those expected from a sample taken from the same population. [b] Primed and unprimed atoms with the same number are related by an inversion center.

$[Mo_2Fe_7S_8(SEt)_{12}]^{3-}$, as evidenced by at least one short Fe···Fe distance (Fe(2)–Fe(3), 2.693 (4) Å) and variations in S···S(4) distances, which range from 3.545 (7) to 3.615 (7) Å. A small irregular distortion, but of a different sort, occurs in $[Mo_2Fe_7S_8(SCH_2Ph)_{12}]^{4-}$, where two of the three Mo···Fe distances are within 3σ and the other (Mo–Fe(3) = 2.717 (2) Å) is somewhat shorter. A similar distortion in $[W_2Fe_7S_8(SCH_2Ph)_{12}]^{4-}$ may be present but the larger esd values in this structure prevent its clear recognition. (6) Excluding the small distortions in (5) and the positions of the benzyl substituents in $[M_2Fe_7S_8(SCH_2Ph)_{12}]^{4-}$, the heavy-atom portion of each cluster in the three anions closely approaches C_{3v} local symmetry. Because the carbon atoms of Fe–SEt substituents in $[Mo_2Fe_7S_8(SEt)_{12}]^{3-}$ lie in core diagonal planes, the entire $MoFe_3S_4(SEt)_3$ cluster in this complex closely conforms to C_{3v} symmetry. (7) Corresponding cluster dimensions in $[Mo_2Fe_7S_8(SCH_2Ph)_{12}]^{4-}$ and $[W_2Fe_7S_8(SCH_2Ph)_{12}]^{4-}$ are within 3σ of each other and thus are of insignificant difference. (8) Corresponding core dimensions and terminal Fe–S distances in the Mo double-cubane complexes $[Mo_2Fe_6S_9(SEt)_8]^{3-}$,[2,3] $[Mo_2Fe_6S_8(SR)_9]^{3-}$ (R = Et,[3] Ph,[4] CH_2CH_2OH[5]), $[Mo_2Fe_7S_8(SEt)_{12}]^{3-}$, and $[Mo_2Fe_7S_8(SCH_2Ph)_{12}]^{4-}$ exhibit no chemically significant differences. Certain other structural characteristics of $MoFe_3S_4(SR)_3$ clusters have been pointed out elsewhere.[3]

Several of the structural features merit further comment. Because the synthesis and properties of Mo–Fe–S and W–Fe–S clusters are being investigated in parallel fashion in this laboratory, a detailed structure of one cluster complex of the latter type was considered desirable. The structural identity of the two $[M_2Fe_7S_8(SCH_2Ph)_{12}]^{4-}$ complexes, feature (7), is consistent with identical or nearly identical six-coordinate radii of Mo and W in the same oxidation state[15] and by a high degree of correspondence in bond distances (excluding M···M separations) in pairs of analogous M(III,IV) complexes; for example, $[M_2Cl_9]^{3-}$,[16] $[M(S_2C_2(CN)_2)_3]^{2-}$,[17] $M_2Cl_2(NMe_2)_4$,[18] $M_2(NMe_2)_6$,[19] $M_2(CH_2SiMe_3)_6$,[20] and $[M(CN)_8]^{4-}$.[21] In addition, there are no important differences in core dimensions of $[M_2Fe_7S_8(SCH_2Ph)_{12}]^{4-}$ and the recently reported (μ-OMe)$_3$ bridged complex $[W_2Fe_6S_8(SPh)_6(OMe)_3]^{3-}$.[22] In complexes of the types **1–4**, any electronic (i.e., oxidation state) differences are essentially localized in the M–[bridge]–M region[3,9] (vide infra), as supported by feature (8). In particular, terminal Fe–SR distances, which measurably respond to oxidation level changes in $[Fe_4S_4(SR)_4]^{2-,3-}$ clusters,[23,24] occur in a narrow interval (2.232 (5)–2.256 (4) Å) in the structures of *all* complexes **1–4** determined in this laboratory. This behavior, together with the near constancy of Fe–S and Fe···Fe distances and of ^{57}Fe isomer shifts (0.27-0.32 mm/s) in Mo and W complexes **1–4**,[3,9,10] provides strong evidence for a nearly invariant structural and electronic environment at the Fe sites regardless of the M oxidation state or the nature of the bridge. On the basis of the previously presented linear relationship between isomer shift and average oxidation state of Fe in tetrahedral Fe-S_4 sites,[3] we favor the $Fe^{2.67+}$ (2Fe(III) + Fe(II)) description in all complexes **1–4**.[25] The origin of the rhombic core distortions in two of the complexes, feature (5), cannot be identified nor can the generality of such distortions be established with only two examples. However, it is observed that $[Fe_4S_4(SR)_4]^{3-}$ clusters which, as individual $M^{III}Fe_3S_4(SR)_3$ clusters, are odd-electron species, exhibit different modes of distortion from idealized cubic core symmetry in the solid state.[24]

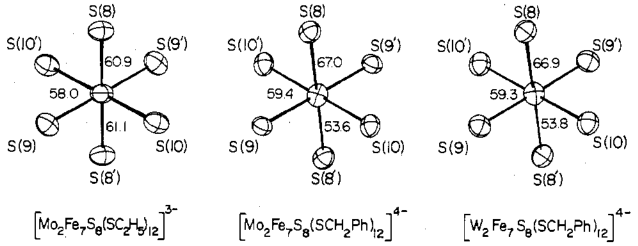

Figure 5. The twist angles ϕ in the Fe^{III}–S_6 bridge subunit of $[Mo_2Fe_7S_8(SEt)_{12}]^{3-}$ and the Fe^{II}–S_6 bridge subunits of $[M_2Fe_7S_8(SCH_2Ph)_{12}]^{4-}$ (M = Mo, W).

B. Bridging Units. The following are the principal structural features of the $M(SR)_3Fe(SR)_3M$ bridging units. (1) Mean M–SR distances in the three anions are insignificantly different from each other and from that in $[Fe_2Mo_6S_8(SEt)_9]^{3-}$ (2.567 (4) Å).[26] (2) Except for M···M and M···Fe(4) separations, all corresponding distances and angles in the two $[M_2Fe_7S_8(SCH_2Ph)_{12}]^{4-}$ complexes are within 3σ, further underscoring the isometric Mo/W relationship observed in cluster structural feature (7). (3) The Fe(4) atom lies on a

---

(15) R. D. Shannon and C. T. Prewitt, *Acta Crystallogr., Sect B*, **25**, 925 (1969); R. D. Shannon, *Acta Crystallogr. Sect. A*, **32**, 751 (1976).

(16) (a) W. H. Watson, Jr., and J. Waser, *Acta Crystallogr.*, **11**, 689 (1958); (b) R. Saillant, R. B. Jackson, W. E. Streib, K. Folting, and R. A. D. Wentworth, *Inorg. Chem.*, **10**, 1453 (1971).

(17) G. F. Brown and E. I. Stiefel, *Inorg. Chem.*, **12**, 2140 (1973).

(18) M. Akiyama, M. H. Chisholm, F. A. Cotton, M. W. Extine, and C. A. Murillo, *Inorg. Chem.*, **16**, 2407 (1977).

(19) M. H. Chisholm, F. A. Cotton, B. A. Frenz, W. W. Reichert, L. W. Shive, and B. R. Stults, *J. Am. Chem. Soc.*, **98**, 4469 (1976); M. H. Chisholm, F. A. Cotton, M. Extine, and B. R. Stults, *ibid.*, **98**, 4477 (1976).

(20) F. Huq, W. Mowat, A. Shortland, A. C. Skapski, and G. Wilkinson, *Chem. Commun.*, 1079 (1971); M. H. Chisholm, F. A. Cotton, M. Extine, and B. R. Stults, *Inorg. Chem.*, **15**, 2252 (1976).

(21) J. L. Hoard, T. A. Hamor, and M. D. Glick, *J. Am. Chem. Soc.*, **90**, 3177 (1968); S. S. Basson, L. D. C. Bok, and J. G. Leipoldt, *Acta Crystallogr., Sect. B*, **26**, 1209 (1970); L. D. C. Bok, J. G. Leipoldt, and S. S. Basson, *Z. Anorg. Allg. Chem.*, **392**, 303 (1972).

(22) G. Christou, C. D. Garner, T. J. King, C. E. Johnson, and J. D. Rush, *J. Chem. Soc., Chem. Commun.*, 503 (1979).

(23) $[Fe_4S_4(SR)_4]^{2-}$: B. A. Averill, T. Herskovitz, R. H. Holm, and J. A. Ibers, *J. Am. Chem. Soc.*, **95**, 3523 (1973); L. Que, Jr., M. A. Bobrik, J. A. Ibers, and R. H. Holm, *ibid.*, **96**, 4168 (1974). See also H. L. Carrell, J. P. Glusker, R. Job, and T. C. Bruice, *ibid.*, **99**, 3683 (1977).

(24) $[Fe_4S_4(SR)_4]^{3-}$: E. J. Laskowski, R. B. Frankel, W. O. Gillum, G. C. Papaefthymiou, J. Renaud, J. A. Ibers, and R. H. Holm, *J. Am. Chem. Soc.*, **100**, 5322 (1978); J. M. Berg, K. O. Hodgson, and R. H. Holm, *ibid.*, **101**, 4586 (1979).

(25) These statements apply only to the trianions of **1**, **2**, and **3** and the tetraanions of **4**. Attempts to isolate reduced forms of these complexes are in progress.

(26) This distance is unavailable for $[Mo_2Fe_6S_9(SEt)_8]^{3-}$ owing to disorder around the crystallographic threefold axis.[2,3]

Table IV. Best Weighted Least-Squares Planes for Anions

plane no.	$Ax + By + Cz = D$ (orthogonalized coordinates)				plane no.	$Ax + By + Cz = D$ (orthogonalized coordinates)			
	A	B	C	D		A	B	C	D
	$(Me_3NCH_2Ph)_3[Mo_2Fe_7S_8(SEt)_{12}]$					$(n\text{-}Bu_4N)_4[Mo_2Fe_7S_8(SCH_2Ph)_{12}]$			
1	0.5852	−0.2520	−0.7707	1.9061	1	0.3496	−0.3342	−0.8753	−0.8873
2	−0.8264	−0.1903	−0.5300	−1.9158	2	−0.9096	0.1429	−0.3900	−12.3861
3	−0.0414	0.9502	−0.3088	−1.9987	3	0.2256	0.9464	−0.2312	5.9283
4	−0.0597	0.9497	−0.3076	−4.1261	4	0.2034	0.9518	−0.2295	3.5874
5	−0.8342	−0.1840	−0.5199	−4.0117	5	−0.9032	0.1262	−0.4103	−14.4631
6	0.5962	−0.2564	−0.7608	4.0159	6	0.3761	−0.3594	−0.8540	1.5366
7	−0.1733	−0.3221	−0.9307	0.0035	7	−0.3989	−0.1555	−0.9037	−9.5427
8	0.3910	0.5000	−0.7727	−0.0618	8	0.4281	0.4368	−0.7912	3.8118
9	−0.5575	−0.8149	−0.1585	0.0688	9	−0.8101	−0.5736	−0.1211	−13.0993
10	−0.6211	0.5340	−0.5736	−4.2483	10	−0.4906	0.7578	−0.4301	−6.1206
11	0.4510	−0.8348	−0.3158	4.2142	11	0.1108	−0.8934	−0.4355	−2.9162
12	0.9848	−0.0553	−0.1646	4.1489	12	0.8851	−0.3376	−0.3204	9.6051

atom	deviations (Å) from plane no.					
	1	2	3	4	5	6
			$(Me_3NCH_2Ph)_3[Mo_2Fe_7S_8(SEt)_{12}]$			
Mo	0.019 (2)	−0.021 (2)	−0.019 (2)			
Fe(1)	0.074 (2)			0.077 (3)	0.085 (3)	
Fe(2)		−0.086 (3)		0.082 (3)		−0.079 (3)
Fe(3)			−0.072 (3)		0.081 (3)	−0.071 (3)
S(1)		0.251 (6)	0.238 (6)			0.247 (5)
S(2)	−0.230 (5)		0.231 (6)		−0.277 (5)	
S(3)	−0.228 (5)	0.242 (5)		−0.249 (6)		
S(4)				−0.290 (6)	−0.321 (6)	0.277 (6)
			$(n\text{-}Bu_4N)_4[Mo_2Fe_7S_8(SCH_2Ph)_{12}]$			
Mo	0.024 (5)	−0.025 (5)	−0.019 (5)			
Fe(1)	0.076 (9)			0.072 (9)	0.085 (9)	
Fe(2)		−0.093 (10)		0.074 (9)		−0.077 (9)
Fe(3)			−0.071 (9)		0.096 (10)	−0.082 (10)
S(1)		0.246 (16)	0.183 (16)			0.225 (16)
S(2)	−0.267 (17)		0.215 (18)		−0.309 (17)	
S(3)	−0.228 (15)	0.245 (16)		−0.223 (17)		
S(4)				−0.287 (19)	−0.355 (18)	0.285 (18)

atom	deviations (Å) from plane no.					
	7	8	9	10	11	12
			$(Me_3NCH_2Ph)_3[Mo_2Fe_7S_8(SEt)_{12}]$			
Mo	−0.003 (2)	0.000 (2)	−0.002 (2)			
Fe(1)			0.005 (3)		−0.001 (3)	−0.006 (3)
Fe(2)		0.002 (3)		−0.007 (3)		0.006 (3)
Fe(3)	0.009 (3)			0.006 (3)	0.001 (3)	
S(1)			0.013 (6)		−0.004 (6)	−0.014 (6)
S(2)		0.004 (5)		−0.015 (6)		0.014 (6)
S(3)	0.021 (5)			0.014 (5)	0.004 (6)	
S(4)	−0.026 (6)	−0.004 (6)	−0.016 (6)			
			$(n\text{-}Bu_4N)_4[Mo_2Fe_7S_8(SCH_2Ph)_{12}]$			
Mo	−0.007 (5)	0.001 (5)	−0.009 (5)			
Fe(1)			0.026 (9)		0.010 (9)	−0.002 (9)
Fe(2)		−0.002 (9)		−0.009 (9)		0.003 (10)
Fe(3)	0.022 (10)			0.009 (10)	−0.011 (9)	
S(1)			0.058 (16)		0.023 (16)	−0.006 (16)
S(2)		−0.006 (17)		−0.022 (17)		0.007 (17)
S(3)	0.044 (15)			0.019 (16)	−0.024 (16)	
S(4)	−0.061 (18)	0.006 (17)	−0.083 (19)			

crystallographically imposed inversion center and occurs in an imperfect trigonal antiprismatic $Fe(SR)_6$ subunit, as seen from these interrelated results: (a) Within sets of Fe–S, S···S, and S···S′ distances and S–Fe–S and S–Fe–S′ angles, values are distinctly unequal and tend to divide into three sets of two as required by the inversion symmetry. (b) The subunits deviate from the dihedral angle shape parameters for a perfect octahedron or D_{3d} trigonal antiprism.[27] Values of one such parameter, the twist angles ϕ formed by projection of Fe–S vectors on a plane perpendicular to the idealized threefold axis and containing the Fe atom, are illustrated for the three anions in Figure 5. For either idealized polyhedron $\phi = 60°$ ($\phi = 0°$ for a D_{3h} trigonal prism). From the collective structural parameters in (a) and (b) the Fe–S_6 subunit much more closely approaches a regular trigonal antiprism in $[Mo_2Fe_7S_8(SEt)_{12}]^{3-}$ than in $[M_2Fe_7S_8(SCH_2Ph)_{12}]^{4-}$. (4) In each anion the highest idealized symmetry of the bridge unit alone,[28] and of all heavy

---

[27] E. L. Muetterties and L. J. Guggenberger, *J. Am. Chem. Soc.*, **96**, 1748 (1974).

[28] The closer approach of bridge unit symmetry to D_{3d} in $[Mo_2Fe_7S_8(SEt)_{12}]^{3-}$ vs. $[M_2Fe_7S_8(SCH_2Ph)_{12}]^{4-}$ is further indicated by the smaller spread of values of S–M–S and M–S–Fe angles (Table III).

Table V. Root-Mean-Square Amplitudes of Thermal Vibration (Å) of Anions

atom	min	int	max
$(Me_3NCH_2Ph)_3[Mo_2Fe_7S_8(SEt)_{12}]$			
Mo	0.183	0.197	0.212
Fe(1)	0.194	0.224	0.249
Fe(2)	0.209	0.245	0.258
Fe(3)	0.190	0.232	0.267
Fe(4)	0.165	0.192	0.224
S(1)	0.192	0.250	0.260
S(2)	0.210	0.220	0.251
S(3)	0.213	0.230	0.248
S(4)	0.188	0.256	0.303
S(5)	0.213	0.267	0.296
S(6)	0.225	0.299	0.395
S(7)	0.208	0.280	0.312
S(8)	0.171	0.200	0.241
S(9)	0.189	0.210	0.234
S(10)	0.177	0.206	0.240
$(n\text{-}Bu_4N)_4[Mo_2Fe_7S_8(SCH_2Ph)_{12}]$			
Mo	0.166	0.191	0.196
Fe(1)	0.181	0.216	0.234
Fe(2)	0.194	0.206	0.227
Fe(3)	0.196	0.209	0.226
Fe(4)	0.172	0.215	0.220
S(1)	0.197	0.211	0.224
S(2)	0.193	0.205	0.238
S(3)	0.185	0.221	0.229
S(4)	0.182	0.230	0.265
S(5)	0.201	0.274	0.285
S(6)	0.211	0.243	0.321
S(7)	0.201	0.247	0.291
S(8)	0.190	0.200	0.217
S(9)	0.175	0.197	0.219
S(10)	0.183	0.192	0.224
$(n\text{-}Bu_4N)_4[W_2Fe_7S_8(SCH_2Ph)_{12}]$			
W	0.177	0.193	0.209
Fe(1)	0.189	0.224	0.248
Fe(2)	0.205	0.212	0.242
Fe(3)	0.204	0.221	0.237
Fe(4)	0.197	0.211	0.228
S(1)	0.203	0.223	0.229
S(2)	0.206	0.216	0.240
S(3)	0.184	0.229	0.236
S(4)	0.190	0.241	0.281
S(5)	0.209	0.276	0.305
S(6)	0.211	0.263	0.331
S(7)	0.209	0.259	0.286
S(8)	0.194	0.223	0.228
S(9)	0.182	0.218	0.227
S(10)	0.193	0.211	0.231

atoms, is D_{3d}. When the positions of all carbon atoms are taken into account, $[Mo_2Fe_7S_8(SEt)_{12}]^{3-}$ closely approaches S_6 symmetry. (5) The differences in bridge unit distances in $[Mo_2Fe_7S_8(SEt)_{12}]^{3-}$ vs. $[M_2Fe_7S_8(SCH_2Ph)_{12}]^{4-}$ can be satisfactorily interpreted in terms of a smaller Fe(III) ion in the former and a larger Fe(II) ion in the latter. From Shannon–Prewitt radii[15] six-coordinate high-spin Fe(II) (0.92 Å) is larger than high-spin (0.79 Å) or low-spin Fe(III) (0.69 Å). In $[Mo_2Fe_7S_8(SEt)_{12}]^{3-}$ the three independent Fe(4)–S distances average 2.309 (9) Å. In $[M_2Fe_7S_8(SCH_2Ph)_{12}]^{4-}$ the corresponding mean distances are substantially longer, 2.567 (6) Å (M = Mo) and 2.566 (1) Å (M = W). The distances between the S(8)–S(9)–S(10) planes and their inversion-related counterparts, 2.95 Å in $[Mo_2Fe_7S_8(SEt)_{12}]^{3-}$ and 3.40 Å (M = Mo) and 3.42 Å (M = W) in $[M_2Fe_7S_8(SCH_2Ph)_{12}]^{4-}$, are further manifestations of the larger bridging atom in the latter complexes.

Bridge structural feature (5) and Mössbauer spectral results[9,10] of Mo and W complexes **3** and **4** are consistent in identifying the bridging Fe atom, instead of a cluster, as the redox site in $[M_2Fe_7S_8(SR)_{12}]^{3-,4-}$ couples.[9,10] Spectra of these complexes consist of two quadrupole doublets in ca. 6:1 intensity ratio. Isomer shifts of the less intense doublet unambiguously correspond to the presence of Fe(III)–S_6 and Fe(II)–S_6 subunits in **3** and **4**, respectively, but do not as clearly identify spin states. With the Shannon–Prewitt radii[15] as a guide, the differences (0.21–0.22 Å) between mean Fe(4)–S distances in $[Mo_2Fe_7S_8(SEt)_{12}]^{3-}$ and $[M_2Fe_7S_8(SCH_2Ph)_{12}]^{4-}$ are inconsistent with low-spin Fe(II) (0.75 Å) in the latter. Indeed, we are unaware of any low-spin Fe(II)–S_6 complexes[29] whereas low-spin Fe(III)–S_6 species, such as $\{Fe[Co(SCH_2CH_2NH_2)_3]_2\}^{3+}$[30] (vide infra), are unexceptional. One expected structural consequence of the larger size of high-spin Fe(II) vs. Fe(III) is not realized. At parity of ligand structure the twist angle ϕ should decrease with increasing metal radius, a behavior observed in low-spin/high-spin Fe(III)–S_6 complexes among many other examples.[27,31,32] In the present cases the differences between the symmetry-related twist angles become larger (Figure 5) but because of the imposed inversion center the average twist angle must be 60°. Apparently, it is energetically advantageous for $(n\text{-}Bu_4N)_4[M_2Fe_7S_8(SCH_2Ph)_{12}]$ to crystallize with imposed centrosymmetry than for the anions to adopt a less distorted structure with $\phi < 60°$.

Bridged complexes of Mo and W with or without direct metal–metal bonds are now entirely common. Structurally defined cases in which M = Mo, W centers are triply bridged include M[X]$_3$M (X = Cl,Br),[16,33] Mo[Cl$_2$(H)]Mo,[34] Mo[(SR)$_3$]Mo,[3-5,35,36] Mo[(SR)$_2$X]Mo (X = S,[2,3] OH,[35] O,[37] Cl[38]), Mo[(OCH$_2$CH$_2$S)X]Mo (X = O,[39] S[40]), and M[(OR)$_3$]M.[22,41] The "extended" triple bridges demonstrated in **3** and **4** are without a proven precedent but are similar to that proposed for $\{Fe[Co(SCH_2CH_2NH_2)_3]_2\}^{3+}$.[30] These bridges suggest some interesting possibilities, such as removal of Fe to afford single clusters which may be of value in further modeling of the Mo site in nitrogenase and a coordination chemistry utilizing these clusters as anionic tripodal ligands. These and other facets of the complexes **3** and **4** are under investigation.

Acknowledgment. This research was supported by NSF Grant No. CHE 77-04397.

Registry No. $(Me_3NCH_2Ph)_3[Mo_2Fe_7S_8(SEt)_{12}]$, 72268-97-4; $(n\text{-}Bu_4N)_4[Mo_2Fe_7S_8(SCH_2Ph)_{12}]$, 72026-39-2; $(n\text{-}Bu_4N)_4[W_2Fe_7S_8(SCH_2Ph)_{12}]$, 72026-38-1.

Supplementary Material Available: Positional and thermal parameters for thiolate carbon atoms of anions (Table VI) and for nitrogen and carbon atoms of cations (Table VII) and values of F_o^2 and F_c^2 for each structure (Tables VIII–X) (63 pages). Ordering information is given on any current masthead page.

---

(29) For examples of high-spin Fe^{II}–S_6 complexes with Mössbauer properties similar to those of **4**, cf. C. A. Yong, B. W. Fitzsimmons, L. F. Larkworthy, and S. E. Al-Mukhtar, *Inorg. Chim. Acta*, **33**, 249 (1979).

(30) G. Freeh, K. Chapman, and E. Blinn, *Inorg. Nucl. Chem. Lett.*, **9**, 91 (1973); R. E. DeSimone, T. Ontko, L. Wardman, and E. L. Blinn, *Inorg. Chem.*, **14**, 1313 (1975).

(31) E. Larsen, G. N. La Mar, B. E. Wagner, J. E. Parks, and R. H. Holm, *Inorg. Chem.*, **11**, 2652 (1972).

(32) A. Avdeef and J. P. Fackler, Jr., *Inorg. Chem.*, **14**, 2002 (1975); D. L. Kepert, *Prog. Inorg. Chem.*, **23**, 1 (1977).

(33) M. G. B. Drew and J. D. Wilkins, *J. Chem. Soc., Dalton Trans.*, 1984 (1975).

(34) A. Bino and F. A. Cotton, *J. Am. Chem. Soc.*, **101**, 4150 (1979).

(35) C. Couldwell, B. Meunier, and K. Prout, *Acta Crystallogr., Sect. B*, **35**, 603 (1979).

(36) I. B. Benson, S. A. R. Knox, P. J. Naish, and A. J. Welch, *J. Chem. Soc., Chem. Commun.*, 878 (1978).

(37) K. Yamanouchi, J. H. Enemark, J. W. McDonald, and W. E. Newton, *J. Am. Chem. Soc.*, **99**, 3529 (1977).

(38) G. Bunzey, J. H. Enemark, J. I. Gelder, K. Yamanouchi, and W. E. Newton, *J. Less-Common Met.*, **54**, 101 (1977).

(39) J. I. Gelder, J. H. Enemark, G. Wolterman, D. A. Boston, and G. P. Haight, *J. Am. Chem. Soc.*, **97**, 1616 (1975).

(40) J. T. Huneke, K. Yamanouchi, and J. H. Enemark, *Inorg. Chem.*, **17**, 3695 (1978).

(41) B. Kanellakopulos, D. Nöthe, K. Weidenhammer, H. Weinand, and M. L. Zeigler, *Angew. Chem., Int. Ed. Engl.*, **16**, 261 (1977).